 FDMP, vol.8, no.3, pp.295-309, 2012

Three-Dimensional Numerical Simulation of Air Cooling of Electronic Components in a Vertical Channel

Y. Amirouche[1] **and R. Bessaïh**[2]

Abstract: This paper summarizes a series of computational results originating from the simulation of three-dimensional turbulent natural convection occurring in a vertical channel containing 5 cubic aluminum heated sources (mimicking a set of electronics components equally spaced in the vertical direction). A three-dimensional, conjugate heat transfer model with appropriate boundary conditions is used. In particular, the governing equations are solved by a finite volume method throughout the entire physical domain. Calculations are made for distinct values of: the Rayleigh number, the ratio (air/solid) of thermal conductivities and other geometrical parameters (in order to examine the influence of such variables on the resulting heat transfer inside the channel).

Keywords: Turbulent, Natural convection, Cooling, Electronic components, Channel.

Nomenclature

B	side of cubic component
D	width of the channel
H	distance between vertical walls
h_e, h_n	heat transfer coefficients
h_s, h_f	on the faces East, North, South and Frontal of the component, respectively
k_{air}	thermal conductivity of air
k_c	thermal conductivity of the component
K	dimensionless turbulent kinetic energy
Q	heat input
q	heat density (heat input per unit volume)
L	length of the plate

[1] University of Jijel, Faculty of Science and Technology, Jijel, Algeria.
[2] University of Mentouri-Constantine, Faculty of Engineering. Department of Mechanical Engineering, Constantine, Algeria.

L_y	distance between the channel inlet and the first block
P	dimensionless pressure
Pr	Prandtl number
Pr_t	turbulent Prandtl number
Ra	Rayleigh number
s	spacing between two consecutive components
T	temperature
t	dimensionless time
U,V,W	dimensionless horizontal, vertical, and transversal velocities, respectively
X,Y,Z	dimensionless horizontal, vertical, and transversal coordinates, respectively
X^*,Y^*,Z^*	horizontal, vertical, and transversal coordinates, respectively

Greek symbols

α	thermal diffusivity coefficient
α_t	turbulent thermal diffusivity
α_t^*	dimensionless turbulent thermal diffusivity
β	thermal expansion coefficient
ε	dimensionless dissipation of the turbulent kinetic energy
κ	Von Karman constant
Θ	dimensionless temperature
ν	kinematic viscosity
ν^*	dimensionless kinematic viscosity
ν_t	turbulent eddy viscosity
ν_t^*	dimensionless turbulent eddy viscosity,
ρ	fluid density

Subscripts

c	component
0	ambient
S	substrate
W	wall

1 Introduction

In many electronic equipments cooling situations, arrays of heat-dissipating components are mounted on vertical parallel plate channels that are open to the ambient at opposite ends. In such a context, difficulties in achieving an efficient cooling of

electronic components are generally considered as the main barriers to developing faster, smaller, and more reliable systems. Indeed, the performance reliability and life expectancy of electronic equipments are inversely related to the components temperature of equipments (Mousa, 2006).

In this paper, "natural" convection is used to cool five electronic components mounted in a vertical channel.

Natural convection heat transfer in a channel was studied by many researchers. For example, Moffat and Ortega (1986) studied natural convection air-cooling of 10 rows and 8 columns of aluminum cubes (heated sources), mounted on an insulated plate. The heat transfer from an array of simulated electronic components for free convection with and without a shrouding wall was experimentally investigated by Ortega and Moffat (1985). Joshi et al. (1989) investigated an experimental study of steady state natural convection from a single column of 8 heated rectangular protrusions. Visualizations in three different vertical planes indicate a three-dimensional, laminar developing boundary region type flow structure away from protrusions. Natural convection in a vertical parallel-wall channel with a single square obstruction was numerically investigated by Said and Muhanna (1990). The components were taken as protruding from one of the two vertical walls forming a channel. Afrid and Zebib (1991) simulated the three-dimensional laminar and turbulent natural convection in a vertical channel, containing ten cubic heated blocks. The results show that the flow rate and the diffusion coefficients are higher in the turbulent flow, resulting in a qualitatively smaller turbulent thermal field, compared to the laminar flow. The work of Desai et al. (1995) concerned cooling in rectangular enclosures with multiple protruding heaters mounted on one side wall, with the top wall being cooled, and the opposing vertical wall and the bottom wall being insulated. Their predictions compared well with previous experimental and numerical work. Huang and Aggarwal (1995) numerically investigated the effects of wall conduction on the cooling of a centered heat source in a two-dimensional rectangular enclosure. Meinders et al. (1998) presented some results of the experimental investigation of the local convective heat transfer from a wall-mounted single array of cubical protrusions along a wall of a wind tunnel. A numerical simulation of conjugate, turbulent natural-convection air cooling of three heated ceramic components mounted on a vertical adiabatic channel was investigated by Bessaïh and Kadja (2000). The results show that the temperature field in each component was found to be almost uniform, and increasing the spacing between the components let to a decrease of their temperature, i.e. better cooling.

The effect of the relative obstacle position on the convective heat transfer from a configuration of two wall-mounted cubes located in channel was studied by Meinders and Hanjalić (2002). Bouterra et al. (2002) studied the turbulent flow around

an obstacle by using the Large Eddy Simulation (L.E.S.) approach of Navier–Stokes equations. Bessaïh and Soudani (2007) simulated the three-dimensional turbulent natural convection air-cooling of 10 cubic aluminum heated sources mounted on a vertical insulating plate. The results show that the better cooling is obtained when the spacing between the heated blocks is increased, and also when the substrate-to-fluid thermal conductivity ratio is very high. Two-dimensional laminar natural convection in a system of parallel vertical channels with a single protruding heat module mounted mid-height on a substrate of finite-thickness was numerically investigated by Desrayaud et al. (2007). Turbulent natural convection of air that happens into inner square cavity with localized heating from horizontal bottom surface was numerically investigated by Brito et al. (2009). Localized heating is simulated by a centrally located heat source on the bottom wall. The average Nusselt number increases with an increase in the Rayleigh number *Ra,* as well as in the dimensionless heat source length. Amirouche and Bessaïh (2010) simulated the three-dimensional laminar mixed convection air-cooling of 10 cubic aluminum heated sources, which are mounted on a vertical channel wall. The results show that a good better cooling is obtained when the Reynolds number is increased and when the spacing between the vertical walls is decreased.

The objective of this study is to determine the effects of the Rayleigh number, the thermal conductivity and the distance between the vertical walls, in order to give qualitative suggestions which may improve the thermal design of printed board assemblies.

2 Geometry and mathematical model

The five aluminum cubes under study are mounted on a vertical channel wall, as illustrated in figure 1. The wall is composed of a layer of 0.44 cm thick Plexiglas upon, which 0.95 cm thick balsa wood planks was epoxied. This geometry is the same as reported in the work of Ortega and Moffat (1985), and Moffat and Ortega (1986). Each cube has a 1.27 cm side (B). The distance between two consecutives heated components is ($S = 2B$). The distance between the channel inlet and the first block (block N°1), and between the last block (block N°5) and the channel exit is L_y (=10cm), which is chosen as length scale. The distance between the vertical walls is ($H = 4B$) and the width of the channel is (D=3B). The length of the channel is L(=36.51cm).

For an incompressible fluid, with constant thermo-physical properties, except for variation of density with temperature in the buoyancy force term (i.e. the Boussinesq approximation is valid), the dimensionless governing equations for the three-dimensional turbulent flow are:

Continuity equation:

$$\frac{\partial U}{\partial X}+\frac{\partial V}{\partial Y}+\frac{\partial W}{\partial Z}=0 \tag{1}$$

Momentum equation in X direction:

$$\frac{\partial U}{\partial t}+\Delta.(\vec{V}U)=-\frac{\partial p}{\partial X}+\mathrm{Pr}\,\Delta.[(\nu^*+\nu_t^*)\Delta U] \tag{2}$$

Momentum equation in Y direction:

$$\frac{\partial V}{\partial t}+\nabla.(\vec{V}V)=-\frac{\partial p}{\partial Y}+\mathrm{Pr}\,\nabla.\left[(\nu^*+\nu_t^*)\nabla V\right]+Ra.\mathrm{Pr}.\Theta \tag{3}$$

Momentum equation in Z direction:

$$\frac{\partial W}{\partial t}+\nabla.(\vec{V}W)=-\frac{\partial p}{\partial Z}+\mathrm{Pr}\,\nabla.\left[(\nu^*+\nu_t^*)\nabla W\right] \tag{4}$$

Energy equation:

$$\frac{\partial \Theta}{\partial t}+\nabla.(\vec{V}\Theta) \quad =\nabla.\left[(k^*+\alpha_t^*)\nabla\Theta\right]+S \tag{5}$$

Turbulent kinetic energy equation:

$$\frac{\partial K}{\partial t}+\nabla.(\vec{V}K)=\mathrm{Pr}\,\nabla.\left[\left(\nu^*+\frac{\nu_t^*}{\sigma_k}\right)\nabla K\right]-\varepsilon-G+P \tag{6}$$

kinetic energy equation rate of dissipation of turbulent:

$$\frac{\partial \varepsilon}{\partial t}+\nabla.(\vec{V}\varepsilon) \quad = \quad \mathrm{Pr}\,\nabla.\left[\left(\nu^*+\frac{\nu_t^*}{\sigma_\varepsilon}\right)\nabla\varepsilon\right]-C_2\varepsilon-C_3G\frac{\varepsilon^2}{K}+C_1\mathrm{P} \tag{7}$$

where

$$P=\mathrm{Pr}\,\nu_t^*\left[\begin{array}{l}\left(\frac{\partial U}{\partial Y}+\frac{\partial V}{\partial X}\right)^2+\left(\frac{\partial V}{\partial Z}+\frac{\partial W}{\partial Y}\right)^2+\left(\frac{\partial W}{\partial X}+\frac{\partial U}{\partial Z}\right)^2+\\ 2\left(\frac{\partial U}{\partial X}\right)^2+2\left(\frac{\partial V}{\partial Y}\right)^2+2\left(\frac{\partial W}{\partial Z}\right)^2\end{array}\right]$$

$$G=Ra\frac{\mathrm{Pr}^2}{\mathrm{Pr}_t}\nu_t^*\frac{\partial\Theta}{\partial Y} \tag{8}$$

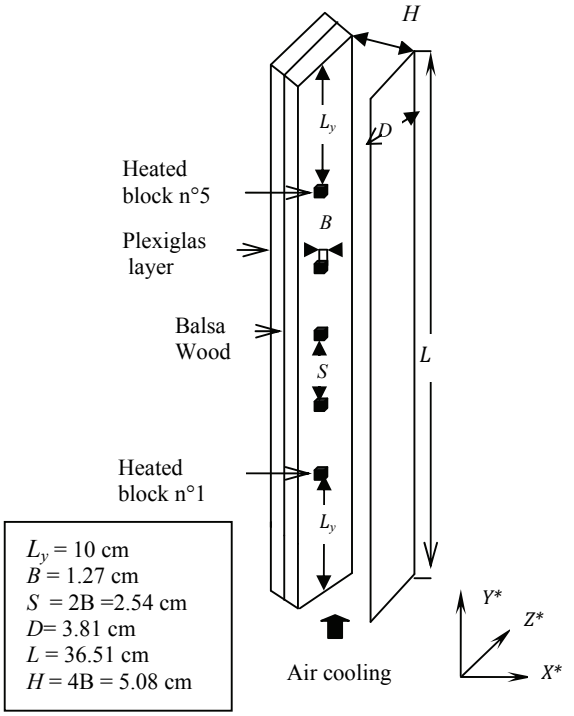

Figure 1: Five cubic heated sources, simulating electronic components, mounted on a vertical channel wall

∇ is the three-dimensional Laplacian operator, $\overrightarrow{V}$ is the dimensionless velocity vector, and U,V,W are the dimensionless components of the velocity vector $\overrightarrow{V}$ in the $X-,Y-$, and Z-directions, respectively, and p is the pressure.

The scales used for the dimensionless of length, time, velocity, pressure, temperature, kinetic energy and dissipation are: $L_y, L_y^2/\alpha$, α/L_y, $\rho(\alpha/L_y)^2$, qL_y^2/k_c, $(\alpha/L_y)^2$, α^3/L_y^4, respectively. *Ra* and *Pr* are the Rayleigh and Prandtl numbers, defined respectively as: $Ra=g\beta(qL_y^5/k_c)/(\nu_{air}.\alpha_{air})$ and $Pr=\nu_{air}/\alpha_{air}$, where q is the heat density, k_c the thermal conductivity of heated components, g the magnitude of gravitational acceleration, β the thermal expansion coefficient of the fluid, ρ its density, ν_{air} the kinematic viscosity, and α_{air} the thermal diffusivity.

In equations 6 and 7, the quantity P represents the production of turbulent kinetic energy due to shear, while G, the production of turbulent kinetic energy due to buoyancy.

The non-dimensional viscosity ν^* is ν/ν_{air} and is equal to 1 in the fluid region

and ∞ within the solid regions .The non-dimensional turbulent eddy viscosity ν_t^* is $(C_\mu/Pr)\ (K^2/\varepsilon)$ in the fluid domain and zero within the solid regions. The non-dimensional thermal conductivity k^* is k/k_{air} and is equal to 1 in the fluid region, k^* =7.25 (for Plexiglas), k^* =2.1 (for Balsa Wood), and k^* = 7846 (for each heated block). The non-dimensional turbulent thermal diffusivity α_t^* is $(Pr/Pr_t)\ \nu_t^*$ in the fluid region and 0 within the solid regions. The energy source S equals 0 for air (no heat generation), and equals 7846 in the heated components. The constants of the standard $(k\text{-}\varepsilon)$ model are: C_1 =1.44;C_2 =1.92;C_μ =0.09; σ_ε =1.30; σ_k =1.00; Pr=0.71 ;Pr_t=1; C_3= 0.70 (Bessaïh and Kadja, 2000).

Initially, at $t = 0,\ U = V = W = \Theta = 0$.

The boundary conditions used for the components of velocity and temperature are:

$$\begin{aligned} &X = 0 :\ U = V = W = 0,\ \frac{\partial \Theta}{\partial X} = 0 \\ &X = \frac{H}{L_y} :\ U = V = W = 0,\ \frac{\partial \Theta}{\partial X} = 0 \end{aligned} \tag{9}$$

$$\begin{aligned} &Y = 0 :\ U = W = 0, \frac{\partial V}{\partial Y} = 0,\ \frac{\partial \Theta}{\partial Y} = 0 \\ &Y = \frac{L}{L_y} :\ \frac{\partial U}{\partial Y} = \frac{\partial V}{\partial Y} = \frac{\partial W}{\partial Y} = 0,\ \frac{\partial \Theta}{\partial Y} = 0 \end{aligned} \tag{10}$$

$$\begin{aligned} &Z = 0 :\ \frac{\partial U}{\partial Z} = \frac{\partial V}{\partial Z} = W = 0,\ \frac{\partial \Theta}{\partial Z} = 0 \\ &Z = \frac{D}{L_y} :\ \frac{\partial U}{\partial Z} = \frac{\partial V}{\partial Z} = W = 0,\ \frac{\partial \Theta}{\partial Z} = 0 \end{aligned} \tag{11}$$

The equations of the turbulent kinetic energy and its dissipation, Eqs. (6) and (7), were solved only in the fluid region. The turbulent kinetic energy is set to zero at solid walls, and its normal gradients are prescribed as zero at the other boundaries. The equation of dissipation is not solved at nodes which are adjacent to the wall; in this region, the production and dissipation of turbulent kinetic energy are equal, which leads to an approximation of the dissipation, $\varepsilon = c_y^{0.75} \frac{K^{1.5}}{\kappa dl}$, where dl is the distance from the wall to the first node, and κ is the von Karman constant and is equal to 0.41(Bessaïh and Kadja, 2000; Ozoe et al., 1986).

3 Numerical method

The governing equations (1)–(7), with the associated boundary conditions are solved using a finite volume technique. The components of the velocity (U,V, and W) are

stored at the staggered locations, and the scalars quantities (p, Θ, K, and ε) are stored in the center of these volumes. A fully implicit time marching scheme is employed. The power law scheme (Patankar, 1980) and the second-order accurate central difference scheme are used to discretize the convection and diffusion fluxes, respectively. The SIMPLER algorithm described by Patankar (1980) are used to determine the pressure from the continuity equation, and the discretized equations were solved iteratively in each direction along the axes using the line-by-line Tri-Diagonal Matrix Algorithm (TDMA). Solutions were considered to be converged, when the maximum of the relative variation in the velocity and scalar quantities between two consecutive dimensionless time steps (Δt= 10^{-4}) is less than 1×10^{-5}, after a sufficiently long marching time, and also when the sum of residuals for all computational cells became negligible (less than 10^{-6}). The total CPU time for the results presented here was about 20 hours.

4 Results and discussion

The independent parameters used in the present work are the Rayleigh number Ra, Prandtl number Pr, thermal conductivity ratio (k_c/k_{air} and k_S/k_{air}), and geometric parameters H/B. The range of independent parameters was chosen and are presented form as follow: Ra =1.82 $\times$ 10^6 and 2.27×10^6, corresponding to 0.8W and 1W heat input, respectively, Pr = 0.71 (for air), k_{air} = 0.026 W/m˚C (for air), k_c/k_{air}= 7846 (for the heated sources), k_S/k_{air} = 7.25 (for Plexiglas), 2.10 (for balsa wood) and 0.10, 10 (for others thermal conductivities considered in this study), and H/B= 2 and 4. The results obtained presented in dimensionless form are shown in figures 2 to 7.

4.1 Grid independence study

The temperature distribution of each heated electronic component for three different grids ($32\times52\times24$, $42\times88\times24$ and $52\times88\times34$) is shown in Figure 2. We find that, the $42\times88\times24$ and $52\times88\times34$ grids lead to a small change of the components temperatures in comparison to the coarse grid $32\times52\times24$. All the results that are presented were obtained with the finer mesh, in order to show as accurate values as possible, since this mesh captures best the dynamic and thermal boundary layers near the solid regions.

4.2 Effect of Rayleigh number (Ra)

In order to reveal important details of the flow structure, the velocity vectors are presented in Figures 3a and 3b for two values of the Rayleigh number, Ra = 1.82×10^6 and 2.27×10^6. In both figures, at the channel inlet the flow field starts with a

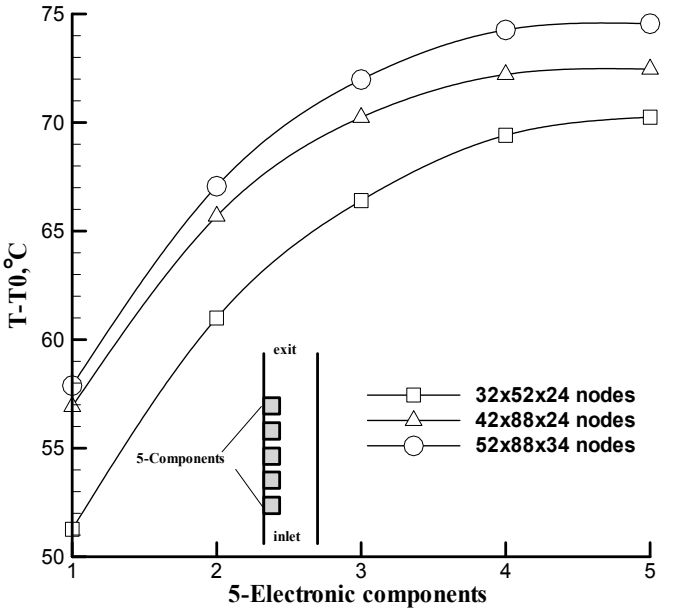

Figure 2: Effect of various grid on the temperature of each heated cubic block for $Ra = 1.82 \times 10^6$($Q = 0.8W$)

parabolic-like velocity profile, the flow velocities along the wall are seen to increase in the vertical direction, especially after the block N°5. In this region, the hot fluid is accelerated resulting in an enhanced heat transfer by convection. At the channel exit, a small diverted flow is observed. This is due to buoyancy: the hot air rises along the relatively channel, whereas the cold air falls along the cold shrouding wall until it is reversed by the stronger incoming main flow.

The effect of Ra on the temperature distribution is shown in Figures 4a-b. It is clear that the temperature increases along the vertical direction (Fig. 4a). We can see that the temperature of each component (Fig. 4b, in °C) becomes constant after the fourth block. This result is confirmed by the experimental work of Ortega and Moffat (1985).

Also, the results presented in Fig. 4a are for the dimensionless temperature $\theta=(T^* - T_0^*)/qL^2/k_c$, which is adimensionlized using the heat density q. This is why the results for $q = 4.87 \times 10^5$ W/m^3 appear to be lower than those for $q = 3.90 \times 10^5$ W/m^3. Through a simple calculation, using Figure 4a, we show that the opposite is true for the dimensional temperature. For example:

For $Q = 1$ W, $q = 4.87 \times 10^5$ W/m^3, $\Theta_{max} = 2.2$; $T_{max} - T_0 = \Theta_{max}.q.L_y^2/k_c$, L_y =10

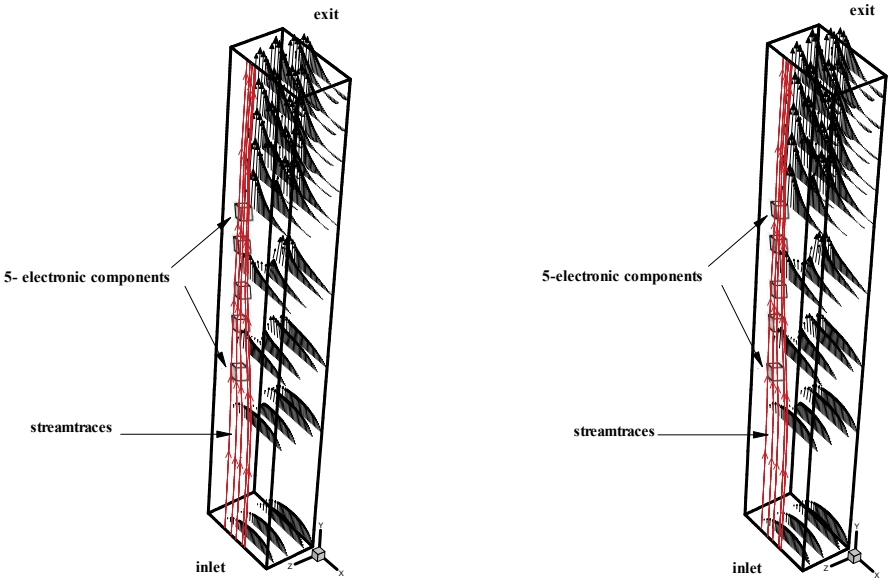

(a) Q=0.8W (Ra=1.82 × 10^6) (b) Q=1W (Ra=2.27 ×10^6)

Figure 3: Vectors plots $(U-V-W)$ in the channel for two values of Q

cm and k_c =204 W/m.˚C,

$T_{max}-T_0$ =2.2× 4.87×10^5×10^{-2}/204 = 52.5 ˚C

For Q =0.8 W, q =3.90×10^5 W/m^3, Θ_{max} =2.35;

$T_{max}-T_0=\Theta_{max}.q.L_y^2/k_c$, L_y =10 cm and k_c =204 W/m.˚C,

$T_{max}-T_0$ =2.35×3.90×10^5×10^2/204= 44.92 ˚C

It is clear from Figures 4a and 4b that for both power inputs considered here (Q =0.8 W and 1 W), the temperature rise between the fifth and fourth block is smaller than that between the fourth and the third block; and between the third and second block is smaller than that between the second and the first block. This is due to the progressive increase of the vertical velocity, which enhances the convective heat transfer coefficient, resulting in more heat removal, and hence results in a good cooling of the blocks.

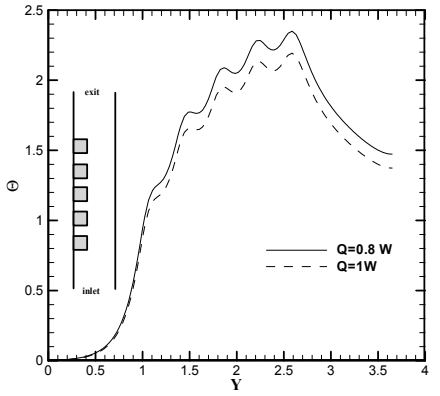

(a) Dimensionless temperature Θ

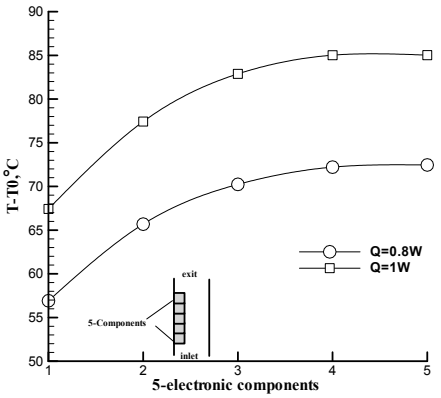

(b) Temperature difference $T\text{-}T_0$, in °C

Figure 4: Temperature distribution for two values of Q

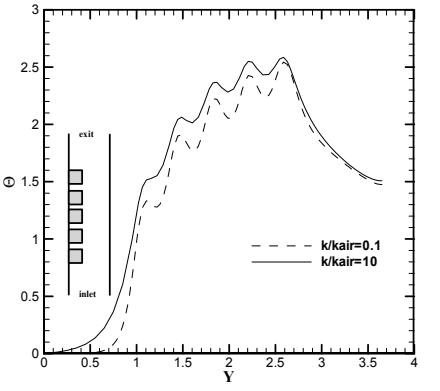

(a) Dimensionless temperature Θ

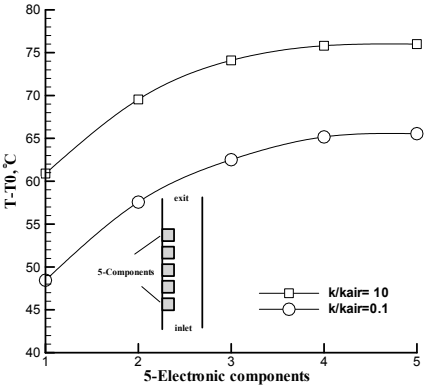

(b) Temperature difference $T\text{-}T_0$, *in* °C

Figure 5: Temperature distribution for two values of k/k_{air}(Q=0.8W)

4.3 Effect of the substrate-to-fluid thermal conductivity ratio (k/k_{air})

The effect of the substrate-to-fluid thermal conductivity ratio (k/k_{air}) on the temperature distribution isshown in Figures 5a and 5b, for two values of thermal conductivity ratio k/k_{air} (0.1 and 10) and $Ra = 1.82\times10^6$, respectively. From Figures 5a and 5b, we note that the dimensional and dimensionless temperatures increase with respect to the thermal conductivity. So, the best cooling is obtained when the thermal conductivity decreases. This result is very important in the cooling of heated electronic component.

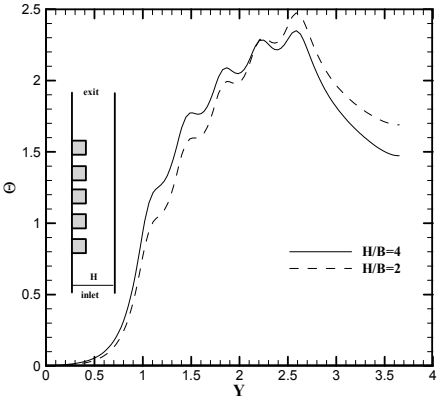

(a) Dimensionless temperature Θ

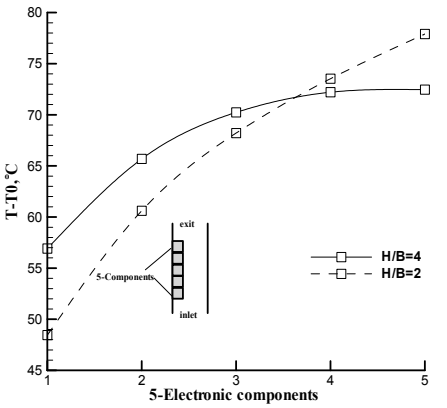

(b) Temperature difference T-T_0, in °C

Figure 6: Temperature distribution for two values of *H/B (Q=0.8W)*

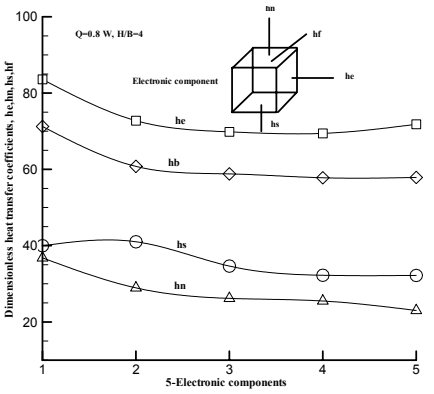

(a) *H/B*=4

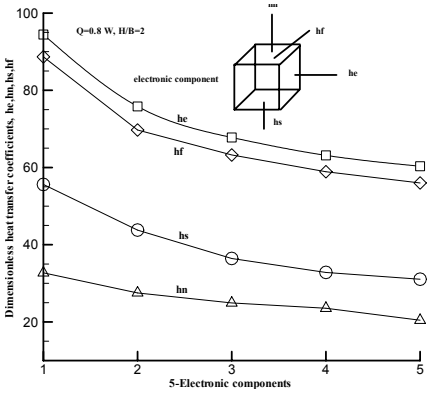

(b) *H/B*=2

Figure 7: Distribution of heat transfer coefficients *h* (*he, hn, hs* and *hf*) of each face of electronics components, for two values of *H/B (Q = 0.8W)*

4.4 Effects of the width (H/B) of the channel

Figures 6a-b illustrate the temperatures distribution Θ (dimensionless values) and$T - T_0$ (dimensional values),and figure 7 shows the heat transfer coefficients for each face of the electronic components ($h_i = Q_i/B^2(T - T_0)$, with i = e, n, s, f) for H/B=2 and 4. For each block, we note that the values of the temperatures increase with the increase of H/B channel, except for blocks 4 and 5. This is due that the blocks 4 and 5 are located near the channel exit, which favors more heat transfer

from the two blocks. The analysis of figures given above and the interpretation of the results show that the buoyant force generally increases with decreasing of the channel width H/B, which causes the increase of heat transfer outside the channel, and therefore the improvement of electronic components cooling.

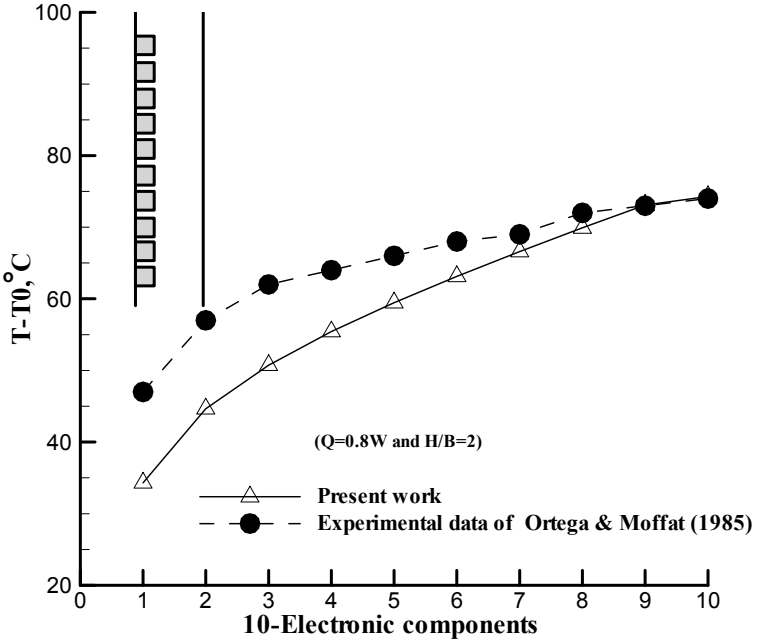

Figure 8: Temperature of each heated component, in ˚C: Comparison between our present numerical simulations and the experimental results of Ortega and Moffat (1985)

4.5 Comparison between our simulations and experimental data

The turbulent natural convection model used in this work has been validated with the experimental data of Ortega and Moffat (1985):the experimental data set and the values of the temperature heated blocks by this model are reported and compared in Figure 8. It is clear that the model of the turbulent natural convection is in good agreement with experimental results from components 7 to 10. However, a difference between electronic components 1 and 6 is shown. This is due probably to the coarse grid used for three-dimensional turbulent natural convection air-cooling of 10 cubic electronic components.

5 Conclusion

Cooling (induced by three-dimensional turbulent natural convection) of five heated electronic components mounted in a vertical channel has been investigated numerically in the framework of a finite-volume method (used to solve the governing mathematical equations).

The temperature field in each component has been found to be almost uniform. The results have been compared with experimental data obtained for similar parameter ranges.

A better cooling is obtained when the Rayleigh number is increased, and when the thermal conductivity and the spacing between the vertical walls of the channel are decreased.

References

Afrid, M.; Zebib, A. (1991): Three-dimensional laminar and turbulent natural convection cooling of heated blocks, *Numerical Heat Transfer, Part A*, vol. 19, pp. 405-424.

Amirouche, Y.; Bessaïh, R. (2010): Three-dimensional laminar mixed convection air-cooling of electronic components mounted on a vertical channel wall, *I.RE.MO.S: International Review on Modelling and Simulations,* vol. 3, no. 1, pp. 116-123.

Bessaïh, R.; Kadja, M. (2000): Turbulent natural convection cooling of electronic components mounted on a vertical channel, *Applied Thermal Engineering*, vol. 20, pp. 141-154.

Bessaïh, R.; Soudani, A. (2007): Numerical simulation of turbulent natural convection air cooling of heated sources mounted in a vertical plate, *Journal of Energy, Heat and Mass Transfer*, vol. 29, pp. 95-117.

Bouterra, M.; Cafsi, A.; Laatar, A.H.; Belghith, A; Le Quéré, P. (2002): Numerical simulation of a stratified two-dimensional dimensional turbulent flow around an obstacle, *Int. J. Thermal Sciences,* vol. 4, pp. 281-293.

Brito, R.F.; Menon, G.J; Pirani, K.J. (2009): Turbulent natural convection in enclosures using large-eddy simulation with localized heating from horizontal bottom surface and cooling from vertical surfaces, , *Journal of the Brazilian Society of Mechanical Sciences and Engineering*, vol. 31, no. 3, pp. 199-209.

Desai, C.P.; Vafai, K.; Keyhani, M. (1995): On the natural convection in a cavity with a cooled top wall and multiple protruding heaters, *ASME J. Electronic Packaging,* vol. 117, pp. 34-45.

Desrayaud, G ; Fichera, A; Lauriat, G. (2007): Natural convection air-cooling

of a substrate-mounted protruding heat source in a stack of parallel boards, *Int. J. Heat Fluid Flow,* vol. 28, pp. 469-482.

Joshi, Y.; Willson, T.; Hazard, S.J. (1989): An experimental study of natural convection from an array of heated protrusions on a vertical surface in water, *ASME J. Electronics Packaging,* vol.111, pp. 121-128.

Huang Y.; Aggarwal K. (1995): Effect of wall conduction on natural convection in an enclosure with a centered heat source, *ASME J. Electronic Packaging,* vol.117, pp. 301-306.

Ozoe, H.; Mouri, A.; Hiramitsu, M.; Churchill, S.W.; Lior, N. (1986): Numerical calculation of three-dimensional turbulent natural convection in a cubical enclosure using a two-equation model of turbulence, *ASME J. Heat Transfer*, vol. 108, pp. 806-813.

Moffat, R.J.; Ortega, A. (1986)**:** Buoyancy induced forced convection, *AIAA/ASME Thermo physics and Heat Transfer Conference,* vol. 57, pp. 135-144, Boston, June 1986, USA.

Meinders, E.R.; Van Der Meer, T.H.; Hanjalić, K. (1998): Local convective heat transfer from an array of wall-mounted cubes, *Int. J. Heat Mass Transfer,* vol.41, pp. 335-346.

Meinders, E.R.; Hanjalić, K. (2002): Experimental study of the convective heat transfer from in-line and staggered configurations of two wall-mounted cubes, *Int. J. Heat and Mass Transfer,* vol.45, pp. 465-482.

Mousa, M.M. (2006): Air cooling characteristics of a uniform square modules array for electronic device heat sink, *Applied Thermal Engineering,* vol. 26, pp. 486-493.

Ortega, A.; Moffat, R.J. (1985): Heat transfer from an array of simulated electronic components: Experimental results for free convection with and without a shrouding wall, *Heat Transfer in Electronic Equipment, ASME HTD,* vol. 48, pp. 5-15.

Patankar, S.V. (1980): *Numerical Heat Transfer and Fluid Flow*, Hemisphere. Washington, DC.

Said, S.A.; Muhanna, A. (1990): Investigation of natural convection in a vertical parallel-walled channel with a single square obstruction, in: A.F. Emery (Ed.), *Simulation and Numerical Methods in Heat Transfer,* vol. 157, ASME: pp. 73-80.